

PDF hosted at the Radboud Repository of the Radboud University Nijmegen

The following full text is a publisher's version.

For additional information about this publication click this link.

<http://hdl.handle.net/2066/128744>

Please be advised that this information was generated on 2020-09-26 and may be subject to change.

Measurements of B meson decays to ωK^* and $\omega\rho$

B. Aubert,¹ R. Barate,¹ D. Boutigny,¹ F. Couderc,¹ Y. Karyotakis,¹ J. P. Lees,¹ V. Poireau,¹ V. Tisserand,¹ A. Zghiche,¹ E. Grauges-Pous,² A. Palano,³ A. Pompili,³ J. C. Chen,⁴ N. D. Qi,⁴ G. Rong,⁴ P. Wang,⁴ Y. S. Zhu,⁴ G. Eigen,⁵ I. Ofte,⁵ B. Stugu,⁵ G. S. Abrams,⁶ A. W. Borgland,⁶ A. B. Breon,⁶ D. N. Brown,⁶ J. Button-Shafer,⁶ R. N. Cahn,⁶ E. Charles,⁶ C. T. Day,⁶ M. S. Gill,⁶ A. V. Gritsan,⁶ Y. Groysman,⁶ R. G. Jacobsen,⁶ R. W. Kadel,⁶ J. Kadyk,⁶ L. T. Kerth,⁶ Yu. G. Kolomoisky,⁶ G. Kukartsev,⁶ G. Lynch,⁶ L. M. Mir,⁶ P. J. Oddone,⁶ T. J. Orimoto,⁶ M. Pripstein,⁶ N. A. Roe,⁶ M. T. Ronan,⁶ W. A. Wenzel,⁶ M. Barrett,⁷ K. E. Ford,⁷ T. J. Harrison,⁷ A. J. Hart,⁷ C. M. Hawkes,⁷ S. E. Morgan,⁷ A. T. Watson,⁷ M. Fritsch,⁸ K. Goetzen,⁸ T. Held,⁸ H. Koch,⁸ B. Lewandowski,⁸ M. Pelizaeus,⁸ T. Schroeder,⁸ M. Steinke,⁸ J. T. Boyd,⁹ N. Chevalier,⁹ W. N. Cottingham,⁹ M. P. Kelly,⁹ T. E. Latham,⁹ F. F. Wilson,⁹ T. Cuhadar-Donszelmann,¹⁰ C. Hearty,¹⁰ N. S. Knecht,¹⁰ T. S. Mattison,¹⁰ J. A. McKenna,¹⁰ D. Thiessen,¹⁰ A. Khan,¹¹ P. Kyberd,¹¹ L. Teodorescu,¹¹ A. E. Blinov,¹² V. E. Blinov,¹² V. P. Druzhinin,¹² V. B. Golubev,¹² V. N. Ivanchenko,¹² E. A. Kravchenko,¹² A. P. Onuchin,¹² S. I. Serednyakov,¹² Yu. I. Skovpen,¹² E. P. Solodov,¹² A. N. Yushkov,¹² D. Best,¹³ M. Bruinsma,¹³ M. Chao,¹³ I. Eschrich,¹³ D. Kirkby,¹³ A. J. Lankford,¹³ M. Mandelkern,¹³ R. K. Mommsen,¹³ W. Roethel,¹³ D. P. Stoker,¹³ C. Buchanan,¹⁴ B. L. Hartfiel,¹⁴ A. J. R. Weinstein,¹⁴ S. D. Foulkes,¹⁵ J. W. Gary,¹⁵ B. C. Shen,¹⁵ K. Wang,¹⁵ D. del Re,¹⁶ H. K. Hadavand,¹⁶ E. J. Hill,¹⁶ D. B. MacFarlane,¹⁶ H. P. Paar,¹⁶ Sh. Rahatlou,¹⁶ V. Sharma,¹⁶ J. W. Berryhill,¹⁷ C. Campagnari,¹⁷ A. Cunha,¹⁷ B. Dahmes,¹⁷ T. M. Hong,¹⁷ A. Lu,¹⁷ M. A. Mazur,¹⁷ J. D. Richman,¹⁷ W. Verkerke,¹⁷ T. W. Beck,¹⁸ A. M. Eisner,¹⁸ C. A. Heusch,¹⁸ J. Kroseberg,¹⁸ W. S. Lockman,¹⁸ G. Nesom,¹⁸ T. Schalk,¹⁸ B. A. Schumm,¹⁸ A. Seiden,¹⁸ P. Spradlin,¹⁸ D. C. Williams,¹⁸ M. G. Wilson,¹⁸ J. Albert,¹⁹ E. Chen,¹⁹ G. P. Dubois-Felsmann,¹⁹ A. Dvoretzki,¹⁹ D. G. Hitlin,¹⁹ I. Narsky,¹⁹ T. Piatenko,¹⁹ F. C. Porter,¹⁹ A. Ryd,¹⁹ A. Samuel,¹⁹ S. Yang,¹⁹ S. Jayatilake,²⁰ G. Mancinelli,²⁰ B. T. Meadows,²⁰ M. D. Sokoloff,²⁰ F. Blanc,²¹ P. Bloom,²¹ S. Chen,²¹ W. T. Ford,²¹ U. Nauenberg,²¹ A. Olivas,²¹ P. Rankin,²¹ J. G. Smith,²¹ K. A. Ulmer,²¹ J. Zhang,²¹ L. Zhang,²¹ A. Chen,²² E. A. Eckhart,²² J. L. Harton,²² A. Soffer,²² W. H. Toki,²² R. J. Wilson,²² Q. Zeng,²² B. Spaan,²³ D. Altenburg,²⁴ T. Brandt,²⁴ J. Brose,²⁴ M. Dickopp,²⁴ E. Feltresi,²⁴ A. Hauke,²⁴ H. M. Lacker,²⁴ R. Müller-Pfefferkorn,²⁴ R. Nogowski,²⁴ S. Otto,²⁴ A. Petzold,²⁴ J. Schubert,²⁴ K. R. Schubert,²⁴ R. Schwierz,²⁴ J. E. Sundermann,²⁴ D. Bernard,²⁵ G. R. Bonneaud,²⁵ F. Brochard,²⁵ P. Grenier,²⁵ S. Schrenk,²⁵ Ch. Thiebaut,²⁵ G. Vasileiadis,²⁵ M. Verderi,²⁵ D. J. Bard,²⁶ P. J. Clark,²⁶ D. R. Lavin,²⁶ F. Muheim,²⁶ S. Playfer,²⁶ Y. Xie,²⁶ M. Andreotti,²⁷ V. Azzolini,²⁷ D. Bettoni,²⁷ C. Bozzi,²⁷ R. Calabrese,²⁷ G. Cibinetto,²⁷ E. Luppi,²⁷ M. Negrini,²⁷ L. Piemontese,²⁷ A. Sarti,²⁷ E. Treadwell,²⁸ F. Anulli,²⁹ R. Baldini-Ferrolì,²⁹ A. Calcaterra,²⁹ R. de Sangro,²⁹ G. Finocchiaro,²⁹ P. Patteri,²⁹ I. M. Peruzzi,²⁹ M. Piccolo,²⁹ A. Zallo,²⁹ A. Buzzo,³⁰ R. Capra,³⁰ R. Contri,³⁰ G. Crosetti,³⁰ M. Lo Vetere,³⁰ M. Macri,³⁰ M. R. Monge,³⁰ S. Passaggio,³⁰ C. Patrignani,³⁰ E. Robutti,³⁰ A. Santroni,³⁰ S. Tosi,³⁰ S. Bailey,³¹ G. Brandenburg,³¹ K. S. Chaisanguanthum,³¹ M. Morii,³¹ E. Won,³¹ R. S. Dubitzky,³² U. Langenegger,³² J. Marks,³² U. Uwer,³² W. Bhimji,³³ D. A. Bowerman,³³ P. D. Dauncey,³³ U. Egede,³³ J. R. Gaillard,³³ G. W. Morton,³³ J. A. Nash,³³ M. B. Nikolich,³³ G. P. Taylor,³³ M. J. Charles,³⁴ G. J. Grenier,³⁴ U. Mallik,³⁴ J. Cochran,³⁵ H. B. Crawley,³⁵ J. Lamsa,³⁵ W. T. Meyer,³⁵ S. Prell,³⁵ E. I. Rosenberg,³⁵ A. E. Rubin,³⁵ J. Yi,³⁵ M. Biasini,³⁶ R. Covarelli,³⁶ M. Pioppi,³⁶ M. Davier,³⁷ X. Giroux,³⁷ G. Grosdidier,³⁷ A. Höcker,³⁷ S. Laplace,³⁷ F. Le Diberder,³⁷ V. Lepeltier,³⁷ A. M. Lutz,³⁷ T. C. Petersen,³⁷ S. Plaszczynski,³⁷ M. H. Schune,³⁷ L. Tantot,³⁷ G. Wormser,³⁷ C. H. Cheng,³⁸ D. J. Lange,³⁸ M. C. Simani,³⁸ D. M. Wright,³⁸ A. J. Bevan,³⁹ C. A. Chavez,³⁹ J. P. Coleman,³⁹ I. J. Forster,³⁹ J. R. Fry,³⁹ E. Gabathuler,³⁹ R. Gamet,³⁹ D. E. Hutchcroft,³⁹ R. J. Parry,³⁹ D. J. Payne,³⁹ C. Touramanis,³⁹ C. M. Cormack,⁴⁰ F. Di Lodovico,⁴⁰ C. L. Brown,⁴¹ G. Cowan,⁴¹ R. L. Flack,⁴¹ H. U. Flaecher,⁴¹ M. G. Green,⁴¹ P. S. Jackson,⁴¹ T. R. McMahon,⁴¹ S. Ricciardi,⁴¹ F. Salvatore,⁴¹ M. A. Winter,⁴¹ D. Brown,⁴² C. L. Davis,⁴² J. Allison,⁴³ N. R. Barlow,⁴³ R. J. Barlow,⁴³ M. C. Hodgkinson,⁴³ G. D. Lafferty,⁴³ A. J. Lyon,⁴³ J. C. Williams,⁴³ A. Farbin,⁴⁴ W. D. Hulsbergen,⁴⁴ A. Jawahery,⁴⁴ D. Kovalskyi,⁴⁴ C. K. Lae,⁴⁴ V. Lillard,⁴⁴ D. A. Roberts,⁴⁴ G. Blaylock,⁴⁵ C. Dallapiccola,⁴⁵ S. S. Hertzbach,⁴⁵ R. Kofler,⁴⁵ V. B. Koptchev,⁴⁵ T. B. Moore,⁴⁵ S. Saremi,⁴⁵ H. Staengle,⁴⁵ S. Willocq,⁴⁵ R. Cowan,⁴⁶ G. Sciolla,⁴⁶ S. J. Sekula,⁴⁶ F. Taylor,⁴⁶ R. K. Yamamoto,⁴⁶ D. J. J. Mangeol,⁴⁷ P. M. Patel,⁴⁷ S. H. Robertson,⁴⁷ A. Lazzaro,⁴⁸ V. Lombardo,⁴⁸ F. Palombo,⁴⁸ J. M. Bauer,⁴⁹ L. Cremaldi,⁴⁹ V. Eschenburg,⁴⁹ R. Godang,⁴⁹ R. Kroeger,⁴⁹ J. Reidy,⁴⁹ D. A. Sanders,⁴⁹ D. J. Summers,⁴⁹ H. W. Zhao,⁴⁹ S. Brunet,⁵⁰ D. Côté,⁵⁰ P. Taras,⁵⁰ H. Nicholson,⁵¹ N. Cavallo,^{52,*} F. Fabozzi,^{52,*} C. Gatto,⁵² L. Lista,⁵² D. Monorchio,⁵² P. Paolucci,⁵² D. Piccolo,⁵² C. Sciacca,⁵² M. Baak,⁵³ H. Bulten,⁵³ G. Raven,⁵³ H. L. Snoek,⁵³ L. Wilden,⁵³ C. P. Jessop,⁵⁴ J. M. LoSecco,⁵⁴ T. Allmendinger,⁵⁵ K. K. Gan,⁵⁵ K. Honscheid,⁵⁵ D. Hufnagel,⁵⁵ H. Kagan,⁵⁵ R. Kass,⁵⁵ T. Pulliam,⁵⁵ A. M. Rahimi,⁵⁵ R. Ter-Antonyan,⁵⁵ Q. K. Wong,⁵⁵ J. Brau,⁵⁶ R. Frey,⁵⁶ O. Igonkina,⁵⁶ M. Lu,⁵⁶ C. T. Potter,⁵⁶ N. B. Sinev,⁵⁶ D. Strom,⁵⁶ E. Torrence,⁵⁶ F. Colechia,⁵⁷ A. Dorigo,⁵⁷ F. Galeazzi,⁵⁷ M. Margoni,⁵⁷ M. Morandin,⁵⁷ M. Posocco,⁵⁷ M. Rotondo,⁵⁷ F. Simonetto,⁵⁷ R. Stroili,⁵⁷ C. Voci,⁵⁷

M. Benayoun,⁵⁸ H. Briand,⁵⁸ J. Chauveau,⁵⁸ P. David,⁵⁸ Ch. de la Vaissière,⁵⁸ L. Del Buono,⁵⁸ O. Hamon,⁵⁸ M. J. J. John,⁵⁸ Ph. Leruste,⁵⁸ J. Malcles,⁵⁸ J. Ocariz,⁵⁸ M. Pivk,⁵⁸ L. Roos,⁵⁸ S. T'Jampens,⁵⁸ G. Therin,⁵⁸ P. K. Behera,⁵⁹ L. Gladney,⁵⁹ Q. H. Guo,⁵⁹ J. Panetta,⁵⁹ C. Angelini,⁶⁰ G. Batignani,⁶⁰ S. Bettarini,⁶⁰ M. Bondioli,⁶⁰ F. Bucci,⁶⁰ G. Calderini,⁶⁰ M. Carpinelli,⁶⁰ F. Forti,⁶⁰ M. A. Giorgi,⁶⁰ A. Lusiani,⁶⁰ G. Marchiori,⁶⁰ M. Morganti,⁶⁰ N. Neri,⁶⁰ E. Paoloni,⁶⁰ M. Rama,⁶⁰ G. Rizzo,⁶⁰ F. Sandrelli,⁶⁰ G. Simi,⁶⁰ J. Walsh,⁶⁰ M. Haire,⁶¹ D. Judd,⁶¹ K. Paick,⁶¹ D. E. Wagoner,⁶¹ N. Danielson,⁶² P. Elmer,⁶² Y. P. Lau,⁶² C. Lu,⁶² V. Miftakov,⁶² J. Olsen,⁶² A. J. S. Smith,⁶² A. V. Telnov,⁶² F. Bellini,⁶³ G. Cavoto,^{62,63} R. Faccini,⁶³ F. Ferrarotto,⁶³ F. Ferroni,⁶³ M. Gaspero,⁶³ L. Li Gioi,⁶³ M. A. Mazzoni,⁶³ S. Morganti,⁶³ M. Pierini,⁶³ G. Piredda,⁶³ F. Safai Tehrani,⁶³ C. Voena,⁶³ S. Christ,⁶⁴ G. Wagner,⁶⁴ R. Waldi,⁶⁴ T. Adye,⁶⁵ N. De Groot,⁶⁵ B. Franek,⁶⁵ N. I. Geddes,⁶⁵ G. P. Gopal,⁶⁵ E. O. Olaiya,⁶⁵ R. Aleksan,⁶⁶ S. Emery,⁶⁶ A. Gaidot,⁶⁶ S. F. Ganzhur,⁶⁶ P.-F. Giraud,⁶⁶ G. Hamel de Monchenault,⁶⁶ W. Kozanecki,⁶⁶ M. Legendre,⁶⁶ G. W. London,⁶⁶ B. Mayer,⁶⁶ G. Schott,⁶⁶ G. Vasseur,⁶⁶ Ch. Yèche,⁶⁶ M. Zito,⁶⁶ M. V. Purohit,⁶⁷ A. W. Weidemann,⁶⁷ J. R. Wilson,⁶⁷ F. X. Yumiceva,⁶⁷ T. Abe,⁶⁸ D. Aston,⁶⁸ R. Bartoldus,⁶⁸ N. Berger,⁶⁸ A. M. Boyarski,⁶⁸ O. L. Buchmueller,⁶⁸ R. Claus,⁶⁸ M. R. Convery,⁶⁸ M. Cristinziani,⁶⁸ G. De Nardo,⁶⁸ D. Dong,⁶⁸ J. Dorfan,⁶⁸ D. Dujmic,⁶⁸ W. Dunwoodie,⁶⁸ S. Fan,⁶⁸ R. C. Field,⁶⁸ T. Glanzman,⁶⁸ S. J. Gowdy,⁶⁸ T. Hadig,⁶⁸ V. Halyo,⁶⁸ C. Hast,⁶⁸ T. Hryn'ova,⁶⁸ W. R. Innes,⁶⁸ M. H. Kelsey,⁶⁸ P. Kim,⁶⁸ M. L. Kocian,⁶⁸ D. W. G. S. Leith,⁶⁸ J. Libby,⁶⁸ S. Luitz,⁶⁸ V. Luth,⁶⁸ H. L. Lynch,⁶⁸ H. Marsiske,⁶⁸ R. Messner,⁶⁸ D. R. Muller,⁶⁸ C. P. O'Grady,⁶⁸ V. E. Ozcan,⁶⁸ A. Perazzo,⁶⁸ M. Perl,⁶⁸ S. Petrak,⁶⁸ B. N. Ratcliff,⁶⁸ A. Roodman,⁶⁸ A. A. Salnikov,⁶⁸ R. H. Schindler,⁶⁸ J. Schwiening,⁶⁸ A. Snyder,⁶⁸ A. Soha,⁶⁸ J. Stelzer,⁶⁸ J. Strube,^{56,68} D. Su,⁶⁸ M. K. Sullivan,⁶⁸ J. Va'vra,⁶⁸ S. R. Wagner,⁶⁸ M. Weaver,⁶⁸ W. J. Wisniewski,⁶⁸ M. Wittgen,⁶⁸ D. H. Wright,⁶⁸ A. K. Yarritu,⁶⁸ C. C. Young,⁶⁸ P. R. Burchat,⁶⁹ A. J. Edwards,⁶⁹ S. A. Majewski,⁶⁹ B. A. Petersen,⁶⁹ C. Roat,⁶⁹ M. Ahmed,⁷⁰ S. Ahmed,⁷⁰ M. S. Alam,⁷⁰ J. A. Ernst,⁷⁰ M. A. Saeed,⁷⁰ M. Saleem,⁷⁰ F. R. Wappler,⁷⁰ W. Bugg,⁷¹ M. Krishnamurthy,⁷¹ S. M. Spanier,⁷¹ R. Eckmann,⁷² H. Kim,⁷² J. L. Ritchie,⁷² A. Satpathy,⁷² R. F. Schwitters,⁷² J. M. Izen,⁷³ I. Kitayama,⁷³ X. C. Lou,⁷³ S. Ye,⁷³ F. Bianchi,⁷⁴ M. Bona,⁷⁴ F. Gallo,⁷⁴ D. Gamba,⁷⁴ L. Bosisio,⁷⁵ C. Cartaro,⁷⁵ F. Cossutti,⁷⁵ G. Della Ricca,⁷⁵ S. Dittongo,⁷⁵ S. Grancagnolo,⁷⁵ L. Lanceri,⁷⁵ P. Poropat,^{75,†} L. Vitale,⁷⁵ G. Vuagnin,⁷⁵ F. Martinez-Vidal,^{2,76} R. S. Panvini,⁷⁷ Sw. Banerjee,⁷⁸ C. M. Brown,⁷⁸ D. Fortin,⁷⁸ P. D. Jackson,⁷⁸ R. Kowalewski,⁷⁸ J. M. Roney,⁷⁸ R. J. Sobie,⁷⁸ J. J. Back,⁷⁹ P. F. Harrison,⁷⁹ G. B. Mohanty,⁷⁹ H. R. Band,⁸⁰ X. Chen,⁸⁰ B. Cheng,⁸⁰ S. Dasu,⁸⁰ M. Datta,⁸⁰ A. M. Eichenbaum,⁸⁰ K. T. Flood,⁸⁰ M. Graham,⁸⁰ J. J. Hollar,⁸⁰ J. R. Johnson,⁸⁰ P. E. Kutter,⁸⁰ H. Li,⁸⁰ R. Liu,⁸⁰ A. Mihalyi,⁸⁰ Y. Pan,⁸⁰ R. Prepost,⁸⁰ P. Tan,⁸⁰ J. H. von Wimmersperg-Toeller,⁸⁰ J. Wu,⁸⁰ S. L. Wu,⁸⁰ Z. Yu,⁸⁰ M. G. Greene,⁸¹ and H. Neal⁸¹

(BABAR Collaboration)

¹Laboratoire de Physique des Particules, F-74941 Annecy-le-Vieux, France

²Universitat Autònoma de Barcelona, E-08193 Bellaterra, Barcelona, Spain

³Università di Bari, Dipartimento di Fisica and INFN, I-70126 Bari, Italy

⁴Institute of High Energy Physics, Beijing 100039, China

⁵University of Bergen, Institute of Physics, N-5007 Bergen, Norway

⁶Lawrence Berkeley National Laboratory and University of California, Berkeley, California 94720, USA

⁷University of Birmingham, Birmingham, B15 2TT, United Kingdom

⁸Ruhr Universität Bochum, Institut für Experimentalphysik I, D-44780 Bochum, Germany

⁹University of Bristol, Bristol BS8 1TL, United Kingdom

¹⁰University of British Columbia, Vancouver, British Columbia, Canada V6T 1Z1

¹¹Brunel University, Uxbridge, Middlesex UB8 3PH, United Kingdom

¹²Budker Institute of Nuclear Physics, Novosibirsk 630090, Russia

¹³University of California at Irvine, Irvine, California 92697, USA

¹⁴University of California at Los Angeles, Los Angeles, California 90024, USA

¹⁵University of California at Riverside, Riverside, California 92521, USA

¹⁶University of California at San Diego, La Jolla, California 92093, USA

¹⁷University of California at Santa Barbara, Santa Barbara, California 93106, USA

¹⁸University of California at Santa Cruz, Institute for Particle Physics, Santa Cruz, California 95064, USA

¹⁹California Institute of Technology, Pasadena, California 91125, USA

²⁰University of Cincinnati, Cincinnati, Ohio 45221, USA

²¹University of Colorado, Boulder, Colorado 80309, USA

²²Colorado State University, Fort Collins, Colorado 80523, USA

²³Universität Dortmund, Institut für Physik, D-44221 Dortmund, Germany

²⁴Technische Universität Dresden, Institut für Kern- und Teilchenphysik, D-01062 Dresden, Germany

- ²⁵*Ecole Polytechnique, LLR, F-91128 Palaiseau, France*
- ²⁶*University of Edinburgh, Edinburgh EH9 3JZ, United Kingdom*
- ²⁷*Università di Ferrara, Dipartimento di Fisica and INFN, I-44100 Ferrara, Italy*
- ²⁸*Florida A&M University, Tallahassee, Florida 32307, USA*
- ²⁹*Laboratori Nazionali di Frascati dell'INFN, I-00044 Frascati, Italy*
- ³⁰*Università di Genova, Dipartimento di Fisica and INFN, I-16146 Genova, Italy*
- ³¹*Harvard University, Cambridge, Massachusetts 02138, USA*
- ³²*Universität Heidelberg, Physikalisches Institut, Philosophenweg 12, D-69120 Heidelberg, Germany*
- ³³*Imperial College London, London, SW7 2AZ, United Kingdom*
- ³⁴*University of Iowa, Iowa City, Iowa 52242, USA*
- ³⁵*Iowa State University, Ames, Iowa 50011-3160, USA*
- ³⁶*Università di Perugia, Dipartimento di Fisica and INFN, I-06100 Perugia, Italy*
- ³⁷*Laboratoire de l'Accélérateur Linéaire, F-91898 Orsay, France*
- ³⁸*Lawrence Livermore National Laboratory, Livermore, California 94550, USA*
- ³⁹*University of Liverpool, Liverpool L69 7ZE, United Kingdom*
- ⁴⁰*Queen Mary, University of London, E1 4NS, United Kingdom*
- ⁴¹*University of London, Royal Holloway and Bedford New College, Egham, Surrey TW20 0EX, United Kingdom*
- ⁴²*University of Louisville, Louisville, Kentucky 40292, USA*
- ⁴³*University of Manchester, Manchester M13 9PL, United Kingdom*
- ⁴⁴*University of Maryland, College Park, Maryland 20742, USA*
- ⁴⁵*University of Massachusetts, Amherst, Massachusetts 01003, USA*
- ⁴⁶*Massachusetts Institute of Technology, Laboratory for Nuclear Science, Cambridge, Massachusetts 02139, USA*
- ⁴⁷*McGill University, Montréal, Quebec City, Canada H3A 2T8*
- ⁴⁸*Università di Milano, Dipartimento di Fisica and INFN, I-20133 Milano, Italy*
- ⁴⁹*University of Mississippi, University, Mississippi 38677, USA*
- ⁵⁰*Université de Montréal, Laboratoire René J. A. Lévesque, Montréal, Quebec City, Canada H3C 3J7*
- ⁵¹*Mount Holyoke College, South Hadley, Massachusetts 01075, USA*
- ⁵²*Università di Napoli Federico II, Dipartimento di Scienze Fisiche and INFN, I-80126, Napoli, Italy*
- ⁵³*NIKHEF, National Institute for Nuclear Physics and High Energy Physics, NL-1009 DB Amsterdam, The Netherlands*
- ⁵⁴*University of Notre Dame, Notre Dame, Indiana 46556, USA*
- ⁵⁵*Ohio State University, Columbus, Ohio 43210, USA*
- ⁵⁶*University of Oregon, Eugene, Oregon 97403, USA*
- ⁵⁷*Università di Padova, Dipartimento di Fisica and INFN, I-35131 Padova, Italy*
- ⁵⁸*Universités Paris VI et VII, Laboratoire de Physique Nucléaire et de Hautes Energies, F-75252 Paris, France*
- ⁵⁹*University of Pennsylvania, Philadelphia, Pennsylvania 19104, USA*
- ⁶⁰*Università di Pisa, Dipartimento di Fisica, Scuola Normale Superiore and INFN, I-56127 Pisa, Italy*
- ⁶¹*Prairie View A&M University, Prairie View, Texas 77446, USA*
- ⁶²*Princeton University, Princeton, New Jersey 08544, USA*
- ⁶³*Università di Roma La Sapienza, Dipartimento di Fisica and INFN, I-00185 Roma, Italy*
- ⁶⁴*Universität Rostock, D-18051 Rostock, Germany*
- ⁶⁵*Rutherford Appleton Laboratory, Chilton, Didcot, Oxon, OX11 0QX, United Kingdom*
- ⁶⁶*DSM/Dapnia, CEA/Saclay, F-91191 Gif-sur-Yvette, France*
- ⁶⁷*University of South Carolina, Columbia, South Carolina 29208, USA*
- ⁶⁸*Stanford Linear Accelerator Center, Stanford, California 94309, USA*
- ⁶⁹*Stanford University, Stanford, California 94305-4060, USA*
- ⁷⁰*State University of New York, Albany, New York 12222, USA*
- ⁷¹*University of Tennessee, Knoxville, Tennessee 37996, USA*
- ⁷²*University of Texas at Austin, Austin, Texas 78712, USA*
- ⁷³*University of Texas at Dallas, Richardson, Texas 75083, USA*
- ⁷⁴*Università di Torino, Dipartimento di Fisica Sperimentale and INFN, I-10125 Torino, Italy*
- ⁷⁵*Università di Trieste, Dipartimento di Fisica and INFN, I-34127 Trieste, Italy*
- ⁷⁶*Universidad de Valencia, E-46100 Burjassot, Valencia, Spain*
- ⁷⁷*Vanderbilt University, Nashville, Tennessee 37235, USA*
- ⁷⁸*University of Victoria, Victoria, British Columbia, Canada V8W 3P6*
- ⁷⁹*Department of Physics, University of Warwick, Coventry CV4 7AL, United Kingdom*
- ⁸⁰*University of Wisconsin, Madison, Wisconsin 53706, USA*
- ⁸¹*Yale University, New Haven, Connecticut 06511, USA*

* Also with Università della Basilicata, Potenza, Italy.

† Deceased.

(Received 16 November 2004; published 15 February 2005)

We describe searches for B meson decays to the charmless vector-vector final states ωK^* and $\omega\rho$ in $89 \times 10^6 B\bar{B}$ pairs produced in e^+e^- annihilation at $\sqrt{s} = 10.58$ GeV. We measure the following branching fractions in units of 10^{-6} : $\mathcal{B}(B^0 \rightarrow \omega K^{*0}) = 3.4^{+1.8}_{-1.6} \pm 0.4 (< 6.0)$, $\mathcal{B}(B^+ \rightarrow \omega K^{*+}) = 3.5^{+2.5}_{-2.0} \pm 0.7 (< 7.4)$, $\mathcal{B}(B^0 \rightarrow \omega\rho^0) = 0.6^{+1.3}_{-1.1} \pm 0.4 (< 3.3)$, and $\mathcal{B}(B^+ \rightarrow \omega\rho^+) = 12.6^{+3.7}_{-3.3} \pm 1.6$. The first error quoted is statistical, the second systematic, and the upper limits are defined at 90% confidence level. For $B^+ \rightarrow \omega\rho^+$ we also measure the longitudinal spin alignment fraction $f_L = 0.88^{+0.12}_{-0.15} \pm 0.03$ and charge asymmetry $\mathcal{A}_{\text{ch}} = (5 \pm 26 \pm 2)\%$.

DOI: 10.1103/PhysRevD.71.031103

PACS numbers: 13.25.Hw, 11.30.Er, 12.15.Hh

The *BABAR* [1–3] and *Belle* [4] experiments have reported observations of B meson decays to most of the charge states of two-body combinations of ρ and K^* mesons. Here we present the results of searches for decays to final states with an ω meson plus a K^* or ρ meson.

The decays $B \rightarrow V_1 V_2$, where V_1 and V_2 are spin-one mesons, proceed through a combination of S -, P -, and D -wave amplitudes or in the helicity basis by amplitudes $A_0, A_{\pm 1}$. The subscripts give the helicities of the vector mesons. The longitudinal A_0 amplitude is a linear combination of S - and D -wave (CP even), while the transverse $A_{\pm 1}$ contain all three partial waves [5].

The spins of the vector mesons are analyzed by their decays into pseudoscalar mesons. We define the helicity frame for each vector meson as its rest frame with polar axis along the direction of the boost from the B rest frame. Because of the limited statistics of the present study we integrate over the azimuthal angles, exploiting the uniform azimuthal acceptance. The angular distribution is

$$\frac{1}{\Gamma} \frac{d^2\Gamma}{d\cos\theta_1 d\cos\theta_2} = \frac{9}{4} \left[\frac{1}{4} (1 - f_L) \sin^2\theta_1 \sin^2\theta_2 + f_L \cos^2\theta_1 \cos^2\theta_2 \right], \quad (1)$$

where θ_k is the decay angle (defined below) in the V_k helicity frame, and $f_L = |A_0|^2 / (|A_{+1}|^2 + |A_0|^2 + |A_{-1}|^2)$ is the fraction of the longitudinal spin component. Measurements in $B \rightarrow \rho\rho$ decays find values close to $f_L = 1$ [1–4], consistent with expectation [6], while smaller values found in $B \rightarrow \phi K^*$ [7] are theoretically puzzling. Since the different angular distributions for the longitudinal and transverse components lead to different acceptances, the f_L dependence needs to be considered in searches as well as in detailed studies of $B \rightarrow V_1 V_2$ decays.

In the decays of B^+ (or the flavor-definite $B^0 \rightarrow K^{*0} X, K^{*0} \rightarrow K^+ \pi^-$) and their charge conjugates it is also of interest to measure the direct-CP-violating charge asymmetry $\mathcal{A}_{\text{ch}} \equiv (\Gamma^- - \Gamma^+) / (\Gamma^- + \Gamma^+)$ in the rates $\Gamma^\pm = \Gamma(B^\pm \rightarrow f^\pm)$ for each final-state f^\pm .

In this study we search for the four decays $B^0 \rightarrow \omega K^{*0}$, $B^+ \rightarrow \omega K^{*+}$, $B^0 \rightarrow \omega\rho^0$, and $B^+ \rightarrow \omega\rho^+$ [8]. A previously published search by CLEO [9] established 90% confidence level (C.L.) upper limits on the branching fractions of $(23, 87, 11, \text{ and } 61) \times 10^{-6}$, respectively.

Because these charmless B decays involve couplings with small Cabibbo-Kobayashi-Maskawa (CKM) mixing matrix elements, several amplitudes potentially contribute with similar strengths, as indicated in Fig. 1. The B^+ modes receive contributions from external tree, color-suppressed tree, and gluonic penguin amplitudes, with the external tree (a) favored for $B^+ \rightarrow \omega\rho^+$, and the penguin (b) strongly favored by CKM couplings for $B^+ \rightarrow \omega K^{*+}$. For the B^0 modes there are no external tree contributions, and again, for $B^0 \rightarrow \omega K^{*0}$ the penguin (c) is CKM favored. For $B^0 \rightarrow \omega\rho^0$ the color-suppressed tree amplitudes (e, f) almost cancel [10] because of the different isospins of the final-state mesons, leaving only a Cabibbo-suppressed penguin (d). Weak exchange and annihilation amplitudes are expected to be negligible.

Theoretical estimates of the branching fractions for vector-vector decays include those based on isospin relations among various modes [11], effective Hamiltonians with factorization and specific B -to-light-meson form factors [10,12–14], and QCD factorization [15]. The estimated branching fractions lie in the range $< 10^{-6}$ (for $B^0 \rightarrow \omega\rho^0$) to 20×10^{-6} (for $B^+ \rightarrow \omega\rho^+$).

The results presented here are based on data collected with the *BABAR* detector [16] at the PEP-II asymmetric e^+e^- collider [17] located at the Stanford Linear Accelerator Center. An integrated luminosity of 81.9 fb^{-1} , corresponding to 88.9 ± 1.0 million $B\bar{B}$ pairs, was recorded at the $Y(4S)$ resonance (center-of-mass energy $\sqrt{s} = 10.58$ GeV).

Charged particles from the e^+e^- interactions are detected, and their momenta measured, by a combination of five layers of double-sided silicon microstrip detectors surrounded by a 40-layer drift chamber, both operating in the 1.5-T magnetic field of a superconducting solenoid. We identify photons and electrons using a CsI(Tl) electromagnetic calorimeter. Further charged particle identification (PID) is provided by the average energy loss (dE/dx) in the tracking devices and by an internally reflecting ring imaging Cherenkov detector covering the central region.

We reconstruct the B -daughter candidates through their decays $\rho^0 \rightarrow \pi^+ \pi^-$, $\rho^+ \rightarrow \pi^+ \pi^0$, $K^{*0} \rightarrow K^+ \pi^- (K_{K^+ \pi^-}^{*0})$, $K^{*+} \rightarrow K^+ \pi^0 (K_{K^+ \pi^0}^{*+})$, $K^{*+} \rightarrow K_S^0 \pi^+ (K_{K_S^0 \pi^+}^{*+})$, $\omega \rightarrow \pi^+ \pi^- \pi^0$, $\pi^0 \rightarrow \gamma\gamma$, and $K_S^0 \rightarrow \pi^+ \pi^-$. Table I lists the requirements on the invariant

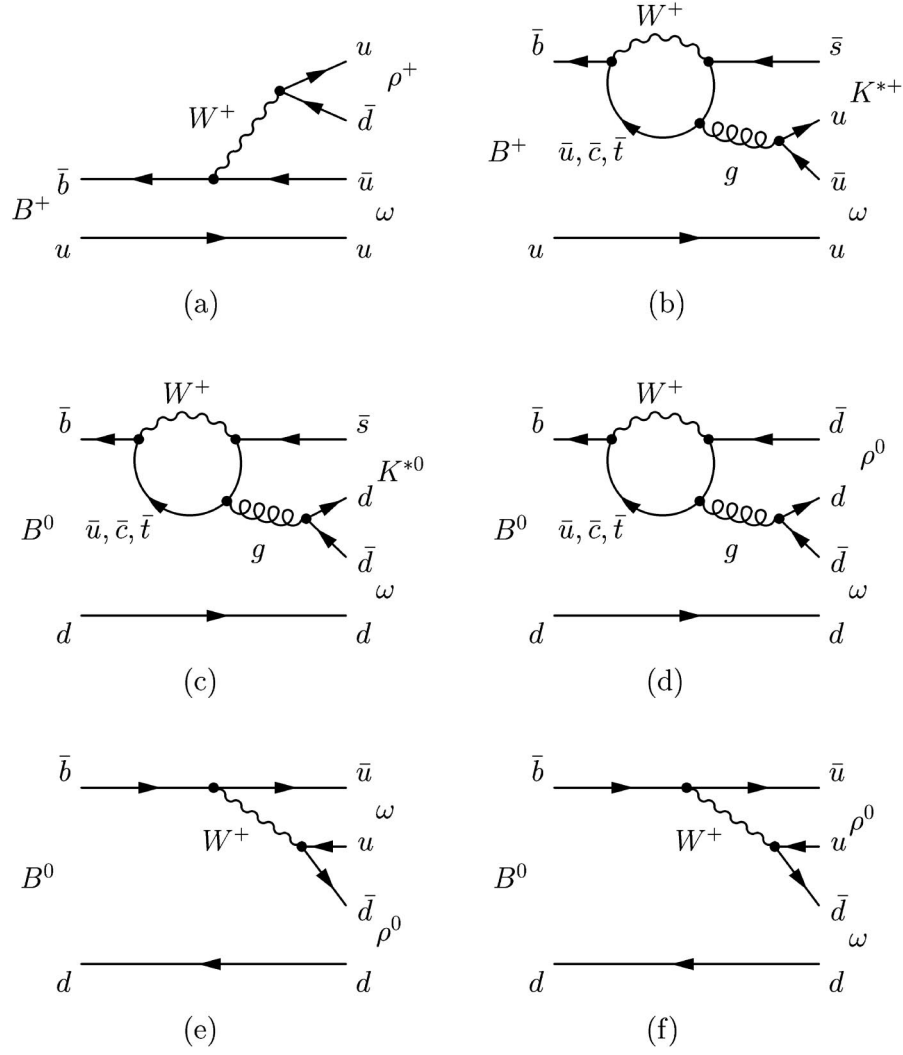


FIG. 1. Representative Feynman diagrams for $B \rightarrow \omega\rho$ and $B \rightarrow \omega K^*$ decays: (a) external tree; (b,c) CKM-favored gluonic penguins; (d) CKM-suppressed penguin; (e,f) destructively interfering color-suppressed trees.

mass of these particles' final states. For the ρ , K^* , and ω invariant masses these requirements are set loose enough to include sidebands, as these mass values are treated as observables in the maximum-likelihood fit described below. For K_S^0 candidates we further require the three-

TABLE I. Selection requirements on the invariant mass (in MeV) and decay angle of B -daughter resonances. The decay angle for ω is unrestricted.

State	inv. mass	decay angle
ρ^0	$510 < m(\pi\pi) < 1060$	$-0.85 < \cos\theta < 0.85$
ρ^+	$470 < m(\pi\pi) < 1070$	$-0.6 < \cos\theta < 0.85$
$K_{K^+ \pi^-}^{*0}, K_{K_S^0 \pi^+}^{*+}$	$755 < m(K\pi) < 1035$	$-0.85 < \cos\theta < 1.0$
$K_{K^+ \pi^0}^{*+}$	$755 < m(K\pi) < 1035$	$-0.6 < \cos\theta < 1.0$
ω	$735 < m(\pi\pi\pi) < 825$	
π^0	$120 < m(\gamma\gamma) < 150$	
K_S^0	$488 < m(\pi\pi) < 508$	

dimensional flight distance from the event primary vertex to be greater than 3 times its uncertainty. Secondary pions and kaons in ρ , K^* , and ω candidates are rejected if their ring imaging Cherenkov detector, dE/dx , and electromagnetic calorimeter PID signature satisfies tight consistency with protons or electrons, and the kaons (pions) must (must not) have a kaon signature.

Table I also gives the restrictions on the K^* and ρ helicity angles θ made to avoid regions of rapid acceptance variation or combinatorial background from soft particles. We define θ as the angle relative to the helicity axis of: the normal to the decay plane for ω , the positively-charged (or only charged) daughter momentum for ρ , and the daughter kaon momentum for K^* .

A B -meson candidate is characterized kinematically by the energy-substituted mass $m_{ES} = [(\frac{1}{2}s + \mathbf{p}_0 \cdot \mathbf{p}_B)^2 / E_0^2 - \mathbf{p}_B^2]^{1/2}$ and energy difference $\Delta E = E_B^* - \frac{1}{2}\sqrt{s}$, where the subscripts 0 and B refer to the initial $\Upsilon(4S)$ and to the B candidate, respectively, and the asterisk denotes the $\Upsilon(4S)$

frame. The resolution on ΔE (m_{ES}) is about 30 MeV (3.0 MeV). We require $|\Delta E| \leq 0.2$ GeV and $5.20 \leq m_{\text{ES}} \leq 5.29$ GeV. The average number of candidates found per selected event is in the range 1.15 to 1.2, depending on the final state. We choose the candidate with the smallest value of a χ^2 constructed from the deviations of the daughter resonance masses from their expected values.

Backgrounds arise primarily from random combinations of particles in continuum $e^+e^- \rightarrow q\bar{q}$ events ($q = u, d, s, c$). We reduce these by selecting on the angle θ_{T} between the thrust axis of the B candidate in the $Y(4S)$ frame and that of the rest of the charged tracks and neutral calorimeter clusters in the event. The distribution of $|\cos\theta_{\text{T}}|$ is sharply peaked near 1.0 for combinations drawn from jetlike $q\bar{q}$ pairs, and nearly uniform for B -meson decays. The requirements, which optimize the expected signal yield relative to its background-dominated statistical error, are $|\cos\theta_{\text{T}}| < 0.8$ for the K^* modes and $|\cos\theta_{\text{T}}| < 0.65$ for the ρ modes. In the maximum-likelihood fit we also use a Fisher discriminant \mathcal{F} [18] that combines four variables defined in the $Y(4S)$ frame: the angles with respect to the beam axis of the B momentum and B thrust axis, and the zeroth and second angular moments $L_{0,2}$ of the energy flow about the B thrust axis. The moments are defined by $L_j = \sum_i p_i \times |\cos\theta_i|^j$, where θ_i is the angle with respect to the B thrust axis of track or neutral cluster i , p_i is its momentum, and the sum excludes the B candidate daughters.

From Monte Carlo (MC) simulation [19] we estimate the residual charmless $B\bar{B}$ background to be 0.1% or less of the total sample in all cases. To allow for contributions possibly missing in the simulation we include a component for these in the fit described below, with a yield free to vary.

We obtain yields, f_L , and \mathcal{A}_{ch} from extended unbinned maximum-likelihood fits with input observables ΔE , m_{ES} , \mathcal{F} , and for vector meson k the mass m_k and helicity-frame decay angle θ_k . For each event i and hypothesis j (signal, continuum background, $B\bar{B}$ background) we define the probability density function (PDF)

$$\mathcal{P}_j^i = \mathcal{P}_j(m_{\text{ES}}^i) \mathcal{P}_j(\Delta E^i) \mathcal{P}_j(\mathcal{F}^i) \mathcal{P}_j(m_1^i, m_2^i, \theta_1^i, \theta_2^i). \quad (2)$$

We check for correlations in the background observables beyond those contained in this PDF and find them to be small. For the signal component, we correct for the effect of neglected correlations (see below). The likelihood function is

$$\mathcal{L} = \frac{e^{-\sum Y_j}}{N!} \prod_{i=1}^N \sum_j Y_j \mathcal{P}_j^i, \quad (3)$$

where Y_j is the yield of events of hypothesis j found by maximizing \mathcal{L} , and N is the number of events in the sample.

The PDF factor for the resonances in the signal takes the form $\mathcal{P}_{1,\text{sig}}(m_1^i) \mathcal{P}_{2,\text{sig}}(m_2^i) \mathcal{Q}(\theta_1^i, \theta_2^i)$ with \mathcal{Q} given by

Eq. (1) modified to account for detector acceptance. For $q\bar{q}$ background it is given for each resonance independently by $\mathcal{P}_{q\bar{q}}(m_k^i, \theta_k^i) = \mathcal{P}_{\text{pk}}(m_k^i) \mathcal{P}_{\text{pk}}(\theta_k^i) + \mathcal{P}_{\text{c}}(m_k^i) \mathcal{P}_{\text{c}}(\theta_k^i)$, distinguishing between true resonance (\mathcal{P}_{pk}) and combinatorial components (\mathcal{P}_{c}). For the $B\bar{B}$ background we take all four mass and helicity-angle observables to be independent. The other PDF forms are sum of two Gaussians for $\mathcal{P}_{\text{sig}}(m_{\text{ES}})$, $\mathcal{P}_{\text{sig}}(\Delta E)$, and the peaking components of $\mathcal{P}_j(m_k)$; a conjunction of two Gaussians with different widths below and above the peak for $\mathcal{P}_j(\mathcal{F})$; and linear or quadratic dependences for ΔE , m_k , and helicity cosines for $q\bar{q}$ combinatorial background. The $q\bar{q}$ background in m_{ES} is described by the function $x\sqrt{1-x^2} \exp[-\xi(1-x^2)]$, with $x \equiv 2m_{\text{ES}}/\sqrt{s}$ and parameter ξ .

For the signal and $B\bar{B}$ background components we determine the PDF parameters from simulation. We study large control samples of B decays to charmed final states of similar topology to verify the simulated resolutions in ΔE and m_{ES} , adjusting the PDFs to account for any differences found. For the continuum background we use (m_{ES} , ΔE) sideband data to obtain initial values, before applying the fit to data in the signal region, and ultimately leave them free to vary in the final fit.

Free parameters of the fit include signal and background yields, background-PDF parameters, and for the mode for which we find a significant signal, f_L and the signal and background charge asymmetries. For the fits without significant signal we fix $f_L = 0.9$, a choice that is consistent with *a priori* expectations, and account for the associated uncertainty in the systematic error. The free background-PDF parameters are ξ for m_{ES} , slope for ΔE , area and slope of the combinatorial component for m_k , and the peak position and lower and upper width parameters for \mathcal{F} .

We evaluate possible biases from our neglect of correlations among discriminating variables in the PDFs by fitting ensembles of simulated experiments into which we have embedded the expected number of signal events randomly extracted from the fully simulated MC samples. We give in Table II the values found for bias for each mode. Events from a weighted mixture of simulated $B\bar{B}$ background decays are included, and so the bias we measure includes the effect of crossfeed from these modes.

In Table II we show for each decay mode the measured branching fraction together with the quantities entering into its computation and with its uncertainty and significance. The statistical error on the signal yield or branching fraction, f_L , and \mathcal{A}_{ch} is taken as the change in the central value when the quantity $-2 \ln \mathcal{L}$ increases by one unit from its minimum value. The significance is taken as the square root of the difference between the value of $-2 \ln \mathcal{L}$ (with systematic uncertainties included) for zero signal and the value at its minimum. For all modes except $B^+ \rightarrow \omega \rho^+$ we quote a 90% C.L. upper limit, taken to be the branching fraction below which lies 90% of the total of the likelihood integral in the positive branching fraction region. In calcu-

TABLE II. Signal yield Y and bias Y_0 with their statistical uncertainties, detection efficiency ϵ , daughter branching fraction product $\prod \mathcal{B}_i$, significance S (with systematic uncertainties included), measured branching fraction \mathcal{B} , and 90% C.L. upper limit for each mode. The number of produced B mesons is $(88.9 \pm 1.0) \times 10^6$.

Mode	Y (events)	Y_0 (events)	ϵ (%)	$\prod \mathcal{B}_i$ (%)	S (σ)	\mathcal{B} (10^{-6})	\mathcal{B} U.L. (10^{-6})
ωK^{*0}	$26.1^{+12.1}_{-10.8}$	3.2 ± 1.1	13.2	59	2.2	$3.4^{+1.8}_{-1.6} \pm 0.4$	6.0
$\omega K^{*+}_{K^0_S \pi^+}$	$11.6^{+8.7}_{-7.2}$	2.9 ± 1.1	13.3	20	1.3	$3.9^{+3.7}_{-3.0} \pm 0.9$...
$\omega K^{*+}_{K^+ \pi^0}$	$5.4^{+6.0}_{-4.2}$	-0.1 ± 0.8	6.7	30	1.4	$3.1^{+3.4}_{-2.4} \pm 0.9$...
ωK^{*+}					1.9	$3.5^{+2.5}_{-2.0} \pm 0.7$	7.4
$\omega\rho^0$	$4.3^{+11.0}_{-9.1}$	-0.5 ± 1.0	10.5	89	0.4	$0.6^{+1.3}_{-1.1} \pm 0.4$	3.3
$\omega\rho^+$	$57.7^{+18.5}_{-16.5}$	4.2 ± 2.8	5.4	89	4.7	$12.6^{+3.7}_{-3.3} \pm 1.6$...

lating branching fractions we assume that the decay rates of the $Y(4S)$ to $B^+ B^-$ and $B^0 \bar{B}^0$ are equal. For decays with K^{*+} , we combine results from the two K^* decay channels by adding the values of $-2 \ln \mathcal{L}$, taking into account the correlated and uncorrelated systematic errors.

We present in Fig. 2 the data and PDFs projected onto m_{ES} and ΔE , for subsamples enriched with a mode-dependent threshold requirement on the ratio of signal to total likelihood (computed without the PDF associated

with the variable plotted) chosen to optimize the significance of signal in the resulting subsample. Figure 3 gives background-subtracted projections onto the helicity-angle cosines for $B^+ \rightarrow \omega\rho^+$ corresponding to the fit result $f_L = 0.88^{+0.12}_{-0.15} \pm 0.03$; the dominance of the term proportional to f_L in Eq. (1) is evident.

The branching fraction value \mathcal{B} given in Table II for $B^+ \rightarrow \omega\rho^+$ comes from a direct fit with the free parameters \mathcal{B} and f_L , as well as \mathcal{A}_{ch} . This choice exploits the

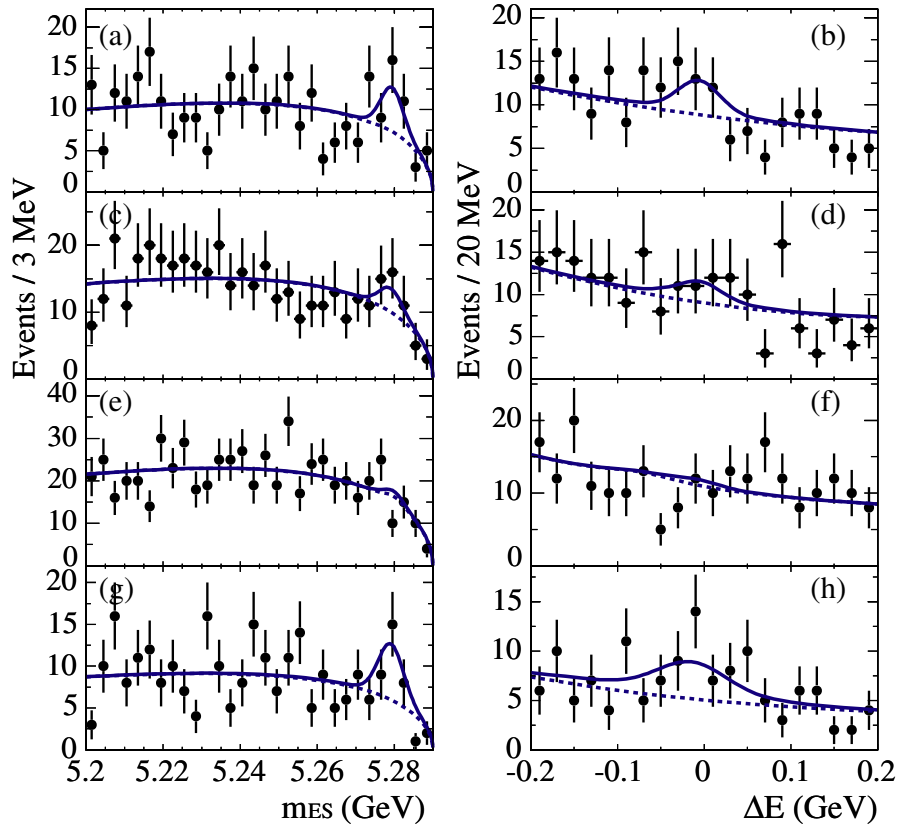


FIG. 2 (color online). Projections of m_{ES} (left) and ΔE (right) with a cut on the per-event signal/total likelihood ratio for (a,b) $B^0 \rightarrow \omega K^{*0}$; (c,d) $B^+ \rightarrow \omega K^{*+}$; (e,f) $B^0 \rightarrow \omega\rho^0$; and (g,h) $B^+ \rightarrow \omega\rho^+$. The solid (dashed) curve gives the total (background) PDF, computed without the variable plotted, and projected onto the same subspace as the data.

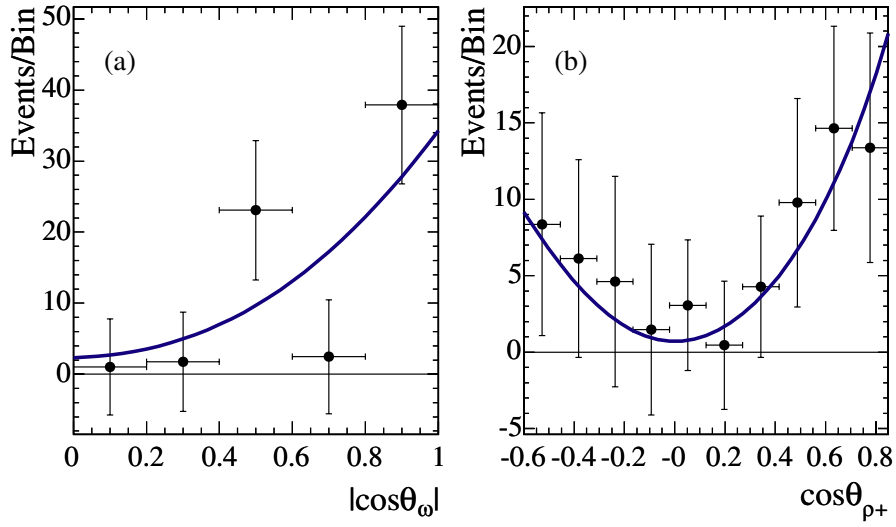


FIG. 3 (color online). Background-subtracted projections of helicity cosines for (a) ω and (b) ρ^+ from the fit for $B^+ \rightarrow \omega\rho^+$.

feature that \mathcal{B} is less correlated with f_L than either the yield or efficiency taken separately. The behavior of $-2\ln\mathcal{L}(f_L, \mathcal{B})$ is shown in Fig. 4.

Most of the systematic uncertainties on the branching fractions arising from lack of knowledge of the PDFs have been included in the statistical error since most background parameters are free in the fit. For the signal, the uncertainties in PDF parameters are estimated from the consistency of fits to MC and data in control modes. Varying the signal-PDF parameters within these errors, we estimate yield uncertainties of 1–4 events, depending on the mode. The uncertainty in the fit-bias correction is taken to be half of the correction itself. Similarly we estimate the uncertainty from modeling the $B\bar{B}$ backgrounds by taking half of the contribution of that component to the fitted signal yield. These additive systematic errors are dominant for the

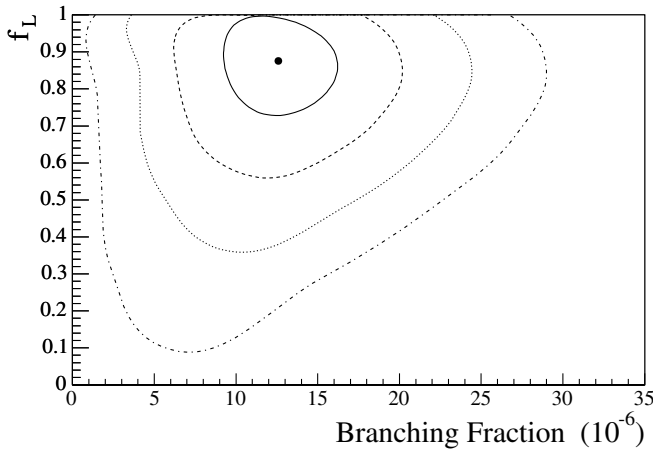


FIG. 4. Distribution of $\chi^2 = -2\ln\mathcal{L}(f_L, \mathcal{B})$ for $B^+ \rightarrow \omega\rho^+$. The solid dot gives the central value; curves give the contours in one-sigma steps ($\Delta\sqrt{\chi^2} = 1$) out to four sigma.

modes with little or no signal yield. We have also considered backgrounds from B decays to the same ultimate final-state as the signal. States with ω and nonresonant $\pi\pi$ or πK are included in the $B\bar{B}$ backgrounds discussed previously. The helicity-angle restrictions given in Table I suppress $\omega\pi$ or ωK subsystems in the region of known resonances. For the $B^0 \rightarrow \omega\rho^0$ and $B \rightarrow \omega K^*$ upper limits, inclusion of the helicity-angle PDF with fixed $f_L = 0.9$ reduces to a negligible level the effect of interferences with possible S wave $\pi\pi$ or πK states.

Uncertainties in our knowledge of the efficiency, found from auxiliary studies, include $0.8\% \times N_i$, $2.5\% \times N_\gamma$, and 4% for a K_S^0 decay, where N_i and N_γ are the number of tracks and photons, respectively, in the B candidate. Our estimate of the B -production systematic error is 1.1%. Published data [20] provide the uncertainties in the B -daughter product branching fractions (1%). The uncertainties in the efficiency from the event selection are 1%–3% for the requirement on $\cos\theta_T$ and 1% for PID for the modes with a charged kaon. The dependence of efficiency on f_L causes uncertainties of 2%–6% in the $B^0 \rightarrow \omega\rho^0$ and $B \rightarrow \omega K^*$ measurements.

The 0.03 systematic error on f_L for $B^+ \rightarrow \omega\rho^+$ comes from imperfect representation of correlations in the PDF and is estimated from fits to fully simulated MC samples. From several large inclusive kaon and B -decay samples, we find a systematic uncertainty for \mathcal{A}_{ch} of 2% due mainly to the dependence of reconstruction efficiency on the charge of the ρ -daughter charged pion. The value of $\mathcal{A}_{\text{ch}}^{qq} = (-1.0 \pm 0.7)\%$ that we find for the background in the $B^+ \rightarrow \omega\rho^+$ fit provides confirmation of this estimate.

In summary, we have performed searches for the previously undetected decays $B^0 \rightarrow \omega K^{*0}$, $B^+ \rightarrow \omega K^{*+}$, $B^0 \rightarrow \omega\rho^0$, and $B^+ \rightarrow \omega\rho^+$. The results are

$$\mathcal{B}(B^0 \rightarrow \omega K^{*0}) = [3.4_{-1.6}^{+1.8} \pm 0.4(<6.0)] \times 10^{-6},$$

$$\mathcal{B}(B^+ \rightarrow \omega K^{*+}) = [3.5_{-2.0}^{+2.5} \pm 0.7(<7.4)] \times 10^{-6},$$

$$\mathcal{B}(B^0 \rightarrow \omega\rho^0) = [0.6_{-1.1}^{+1.3} \pm 0.4(<3.3)] \times 10^{-6},$$

$$\mathcal{B}(B^+ \rightarrow \omega\rho^+) = (12.6_{-3.3}^{+3.7} \pm 1.6) \times 10^{-6},$$

where the first error quoted is statistical, the second systematic, and the upper limits are taken at 90% C.L. For $B^+ \rightarrow \omega\rho^+$ we also measure the longitudinal polarization fraction

$$f_L = 0.88_{-0.15}^{+0.12} \pm 0.03,$$

and charge asymmetry

$$\mathcal{A}_{\text{ch}} = (5 \pm 26 \pm 2)\%.$$

We find that the longitudinal spin alignment is dominant, as for the $\rho\rho$ modes [1–4]. The central value of the

branching fraction for $B^+ \rightarrow \omega\rho^+$ is about half of those found for $B^+ \rightarrow \rho^+\rho^0$ and $B^0 \rightarrow \rho^+\rho^-$. All of our branching fraction results are in general agreement within errors with the theoretical estimates.

We are grateful for the excellent luminosity and machine conditions provided by our PEP-II colleagues and for the substantial dedicated effort from the computing organizations that support *BABAR*. The collaborating institutions wish to thank SLAC for its support and kind hospitality. This work is supported by DOE and NSF (USA), NSERC (Canada), IHEP (China), CEA and CNRS-IN2P3 (France), BMBF and DFG (Germany), INFN (Italy), FOM (The Netherlands), NFR (Norway), MIST (Russia), and PPARC (United Kingdom). Individuals have received support from CONACyT (Mexico), A. P. Sloan Foundation, Research Corporation, and Alexander von Humboldt Foundation.

-
- [1] *BABAR* Collaboration, B. Aubert *et al.*, Phys. Rev. Lett. **91**, 171 802 (2003).
 [2] *BABAR* Collaboration, B. Aubert *et al.*, Phys. Rev. D **69**, 031102 (2004).
 [3] *BABAR* Collaboration, B. Aubert *et al.*, Phys. Rev. Lett. **93**, 231 801 (2004).
 [4] BELLE Collaboration, J. Zhang *et al.*, Phys. Rev. Lett. **91**, 221 801 (2003).
 [5] Amol S. Dighe *et al.*, Phys. Lett. B **369**, 144 (1996).
 [6] A. Ali *et al.*, Z. Phys. C **1**, 269 (1979); M. Suzuki, Phys. Rev. D **66**, 054018 (2002).
 [7] *BABAR* Collaboration, B. Aubert *et al.*, Phys. Rev. Lett. **91**, 171 802 (2003); BELLE Collaboration, K.-F. Chen *et al.*, Phys. Rev. Lett. **91**, 201 801 (2003).
 [8] Charge-conjugate reactions are included implicitly.
 [9] CLEO Collaboration T. Bergfeld *et al.*, Phys. Rev. Lett. **81**, 272 (1998).
 [10] A. Ali, G. Kramer, and C. D. Lu, Phys. Rev. D **58**, 094009 (1998).
 [11] D. Atwood and A. Soni, Phys. Rev. D **59**, 013007 (1999).
 [12] Y. H. Chen *et al.*, Phys. Rev. D **60**, 094014 (1999).
 [13] A. Ali, G. Kramer, and C. D. Lu, Phys. Rev. D **59**, 014005 (1999).
 [14] W.-S. Hou and K.-C. Yang, Phys. Rev. D **61**, 073014 (2000).
 [15] H.-Y. Chang and K.-C. Yang, Phys. Lett. B **511**, 40 (2001).
 [16] *BABAR* Collaboration, B. Aubert *et al.*, Nucl. Instrum. Methods Phys. Res., Sect. A **479**, 1 (2002).
 [17] PEP-II Collaboration, Stanford Linear Accelerator Center Report No. SLAC-R-418 (1993).
 [18] R. A. Fisher, Ann. Eugenics **7**, 179 (1936).
 [19] The *BABAR* detector Monte Carlo simulation is based on GEANT4: S. Agostinelli *et al.*, Nucl. Instrum. Methods Phys. Res., Sect. A **506**, 250 (2003).
 [20] Particle Data Group, S. Eidelman *et al.*, Phys. Lett. B **592**, 1 (2004).